Journal of Geophysical Research – Space Physics

Supporting Information for

Statistical study of ion upflow and downflow observed by the Poker Flat Incoherent Scatter Radar (PFISR)

Jiaen Ren[1], Shasha Zou[1], Jiayue Lu[2], Naomi Giertych[3], Yang Chen[3], Roger H. Varney[4], Ashton S. Reimer[4]

[1]Department of Climate and Space Sciences and Engineering, College of Engineering, University of Michigan, Ann Arbor, Michigan

[2]Department of Computer Science, College of Literature, Science, and the Arts, University of Michigan, Ann Arbor, Michigan

[3]Department of Statistics, College of Literature, Science, and the Arts, University of Michigan, Ann Arbor, Michigan

[4]Center for Geospace Studies, SRI International, Menlo Park, California, USA

Contents of this file

Text T1. A more restrict data selection method has been tested and the results are shown in Figures S1-S14. First, we have the same data quality control criteria that the ratio between the velocity measurement uncertainty and the magnitude of the measurement itself must be smaller than one unless the uncertainty is less than 100 m/s. Second, we select reliable ion upflow/downflow events when there are at least three consecutive ion field-aligned speed, **after minus/plus measurement uncertainty**, larger/smaller than 100/-100 m/s in the velocity altitude profile.

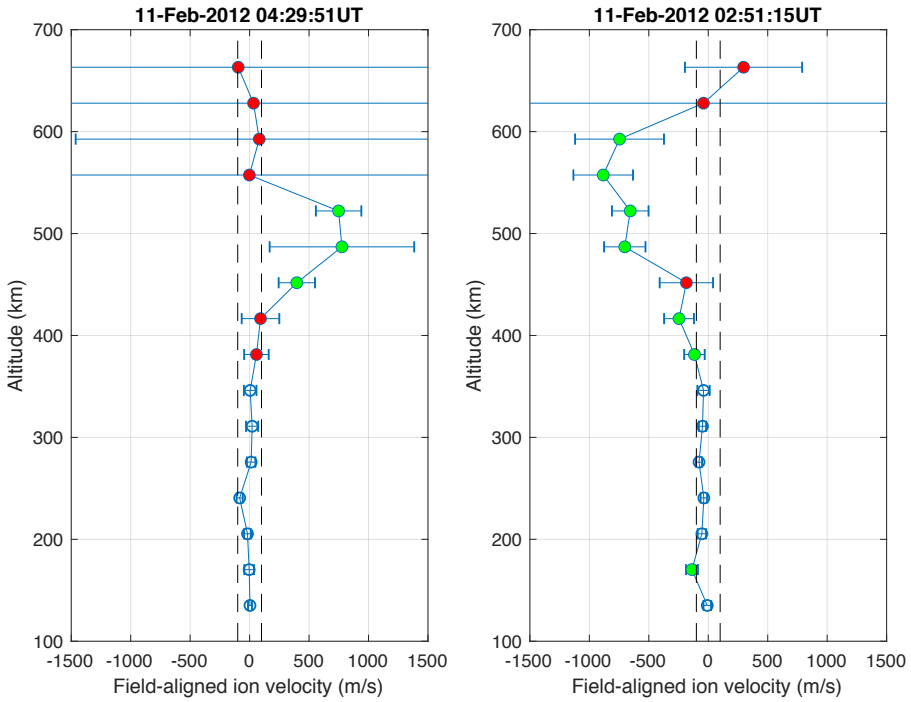

Figure S1. Examples of identified ion upflow and downflow events. The left and right panel shows examples of an ion upflow record and an downflow record, respectively, on February 11, 2012. The dashed vertical lines mark -100/100 m/s field-aligned ion velocity. The dots in red mark the invalid data points that don't satisfy the data quality criteria, while those in green indicate all the valid data points with velocity smaller/larger than -100/100 m/s for downflow/upflow. Profiles with at least 3 consecutive green dots are selected as downflow/upflow events.

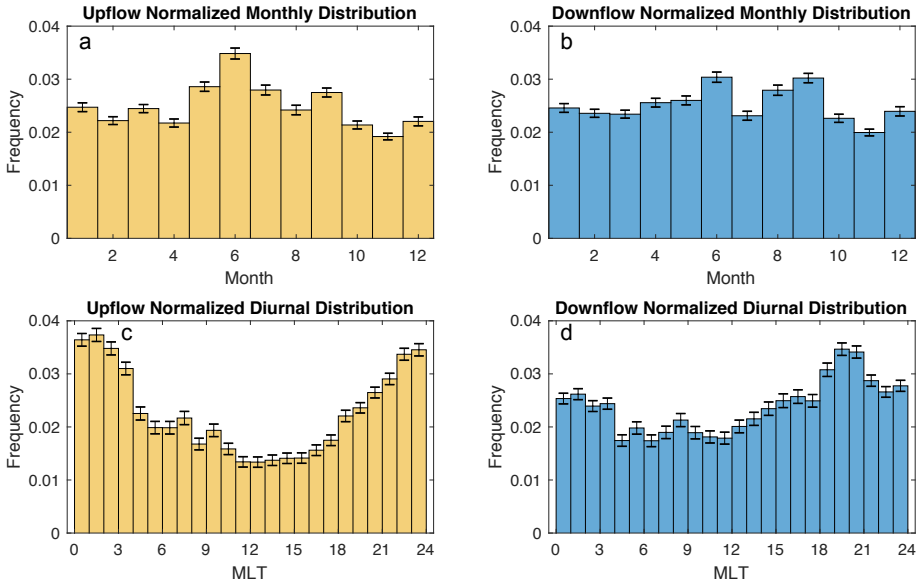

Figure S2. Monthly distribution of ion upflow (a) and downflow (b) occurrence frequencies. Magnetic local time (MLT) distribution of ion upflow (c) and downflow (d) occurrence frequencies. MLT is universal time (UT) + 13 at the PFISR site.

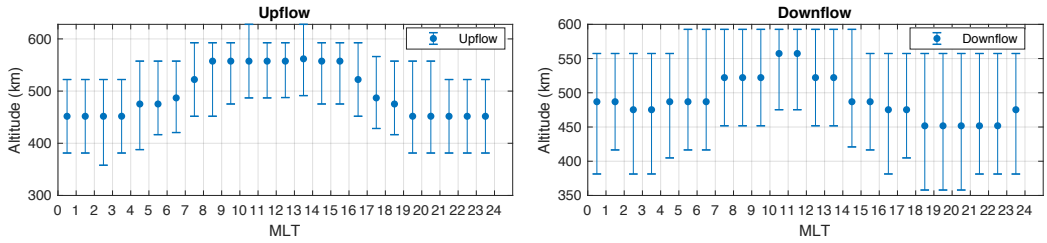

Figure S3. Average altitudes of ion (a) upflow and (b) downflow observed by PFISR at each MLT. The dots mark the median altitude of upflows/downflows observed within each MLT bin, while the vertical bars indicate the interquartile range from 25% to 75%.

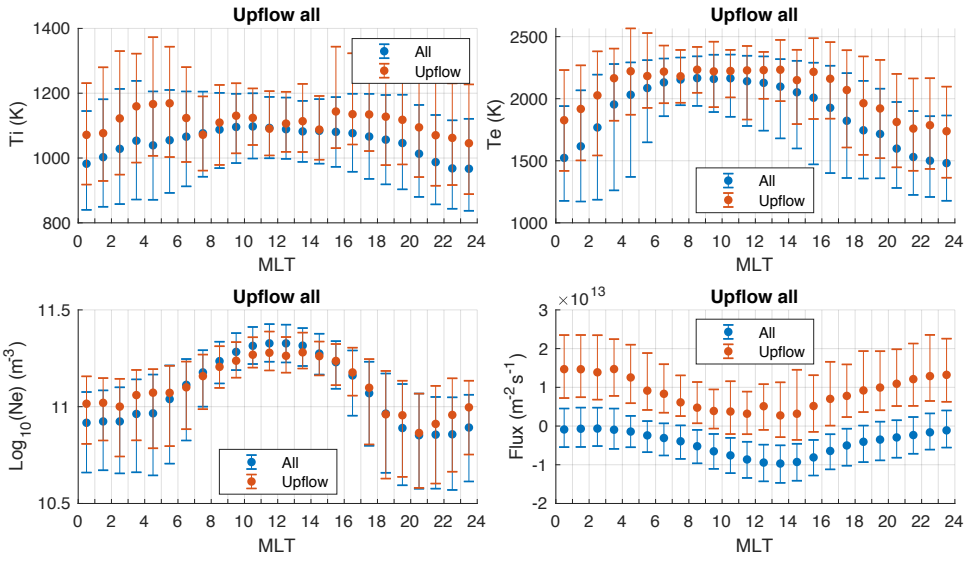

Figure S4. Distribution of (a) ion and (b) electron temperature, (c) electron density and (d) field-aligned ion flux, averaged below 600 km, as a function of MLT with only ion upflow profiles and with all the profiles. The upflow flux is averaged over altitudes where the upflow

occurs. The dots mark the median value for each bin and the vertical bars indicate the interquartile range from 25% to 75%.

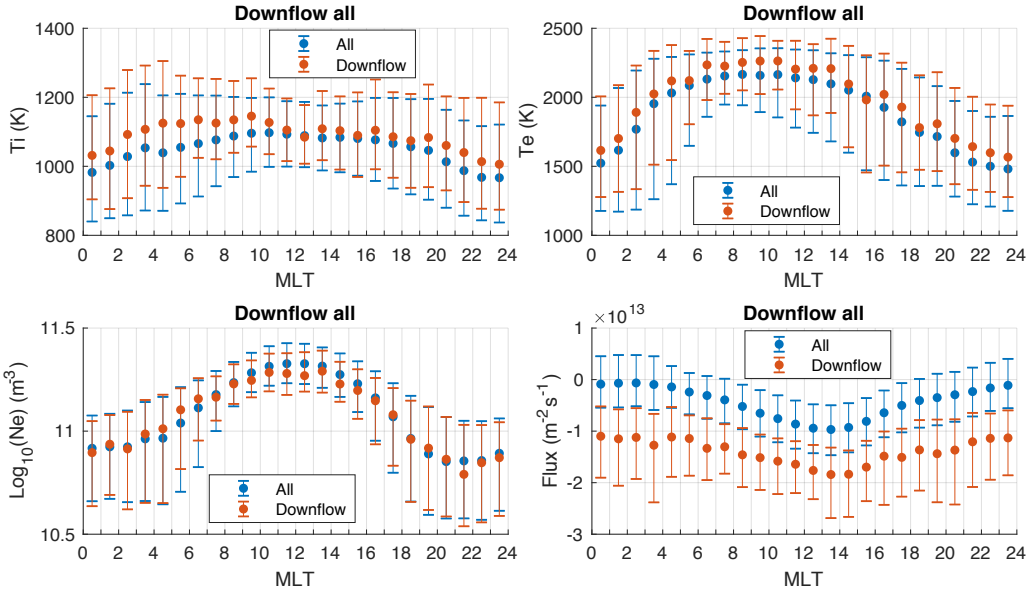

Figure S5. Distribution of (a) ion and (b) electron temperature, (c) electron density and (d) field-aligned ion flux, averaged below 600 km, as a function of MLT with only ion downflow profiles and with all the profiles. The downflow flux is averaged over altitudes where the downflow occurs. The dots mark the median value for each bin and the vertical bars indicate the interquartile range from 25% to 75%.

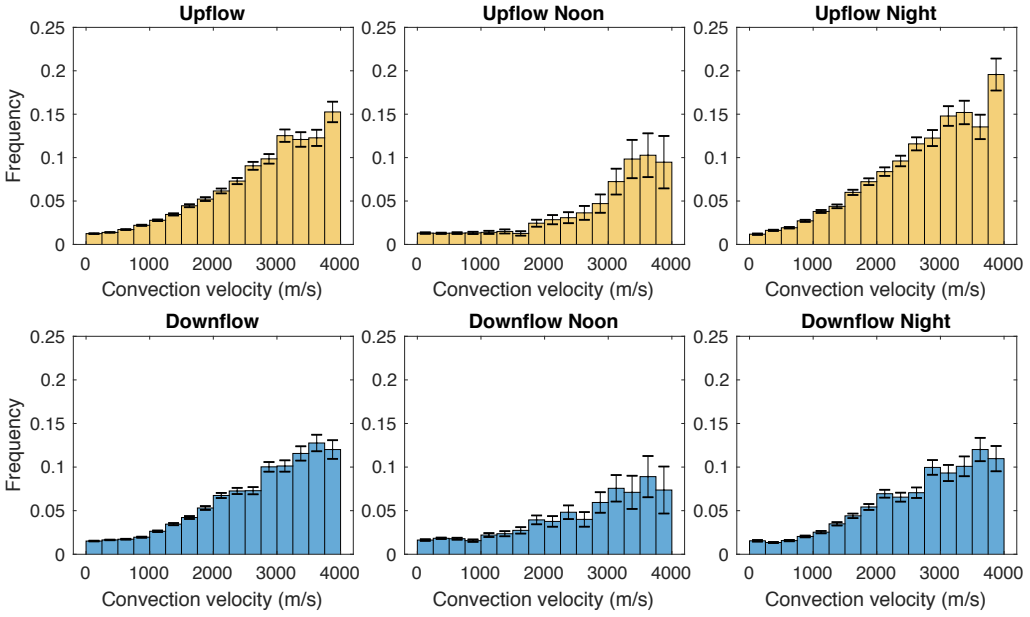

Figure S6. Occurrence frequency of ion upflow and downflow as a function of ion convection velocity for different MLT intervals: (a) all MLTs, (b) on the dayside between 9 – 15 MLT (1244

upflows, 1666 downflows), (c) on the nightside between 21 – 3 MLT (5001 upflows, 3861 downflows). Downflow occurrence frequencies are in the same format as that for upflow.

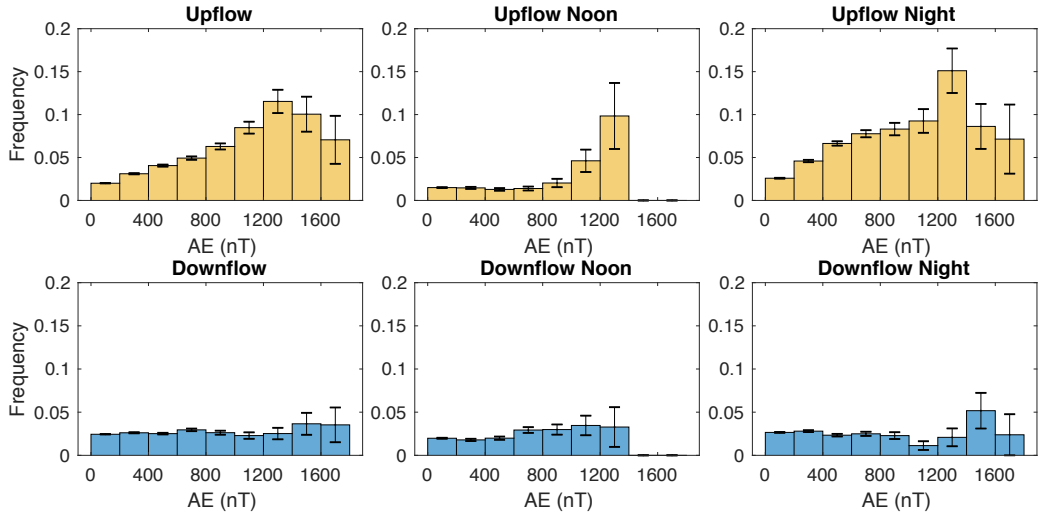

Figure S7. Ion upflow (first row) occurrence frequency plotted over AE index over different MLT intervals: (a) all MLTs, (b) on the dayside between 9 – 15 MLT (1244 upflows, 1666 downflows), (c) on the nightside between 21 – 3 MLT (5001 upflows, 3861 downflows). Downflow occurrence frequency (second row) formats the same as upflow.

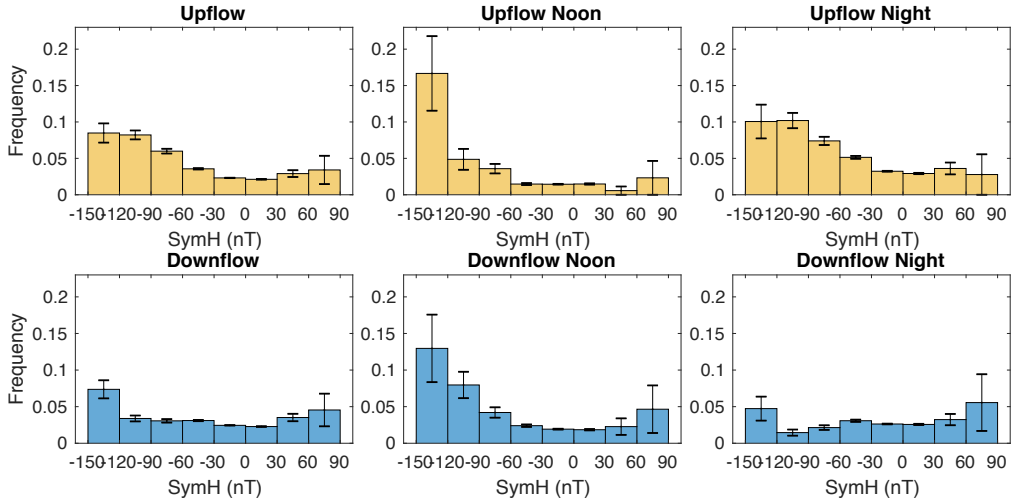

Figure S8. Ion upflow (first row) occurrence frequency plotted over SymH index over different MLT intervals: (a) all MLTs, (b) on the dayside between 9 – 15 MLT (1244 upflows, 1666

downflows), (c) on the nightside between 21 – 3 MLT (5001 upflows, 3861 downflows). Downflow occurrence frequency (second row) formats the same as upflow.

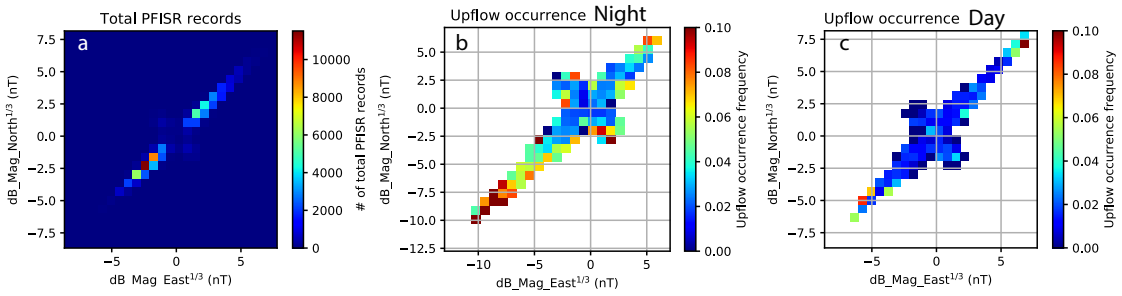

Figure S9. Heatmaps showing (a) distributions of local magnetic puerturbations matched with all PFISR records, (b and c) distribution of ion upflow occurrence frequency on local magnetic perturbations for data on the (b) night side between 21 – 3 MLT and (c) on the dayside between 9 – 15 MLT. The magnetic perturbations are measured in local magnetic north and east directions and are plotted after applying cubic root for better visual clarity.

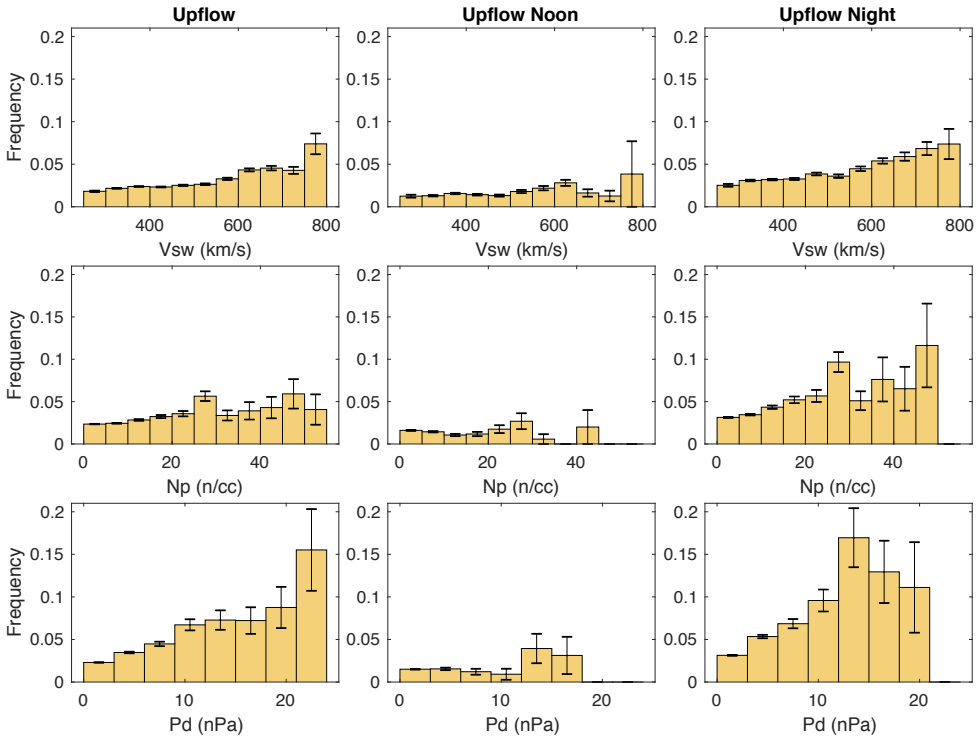

Figure S10. Ion upflow occurrence frequency plotted over solar wind parameters: velocity (first row), proton number density (second row), dynamic pressure (third row), for different

MLT intervals: Over all MLT (first column), over noon sector, 9 – 15 MLT (second column), over midnight sector, 21 – 3 MLT (third column).

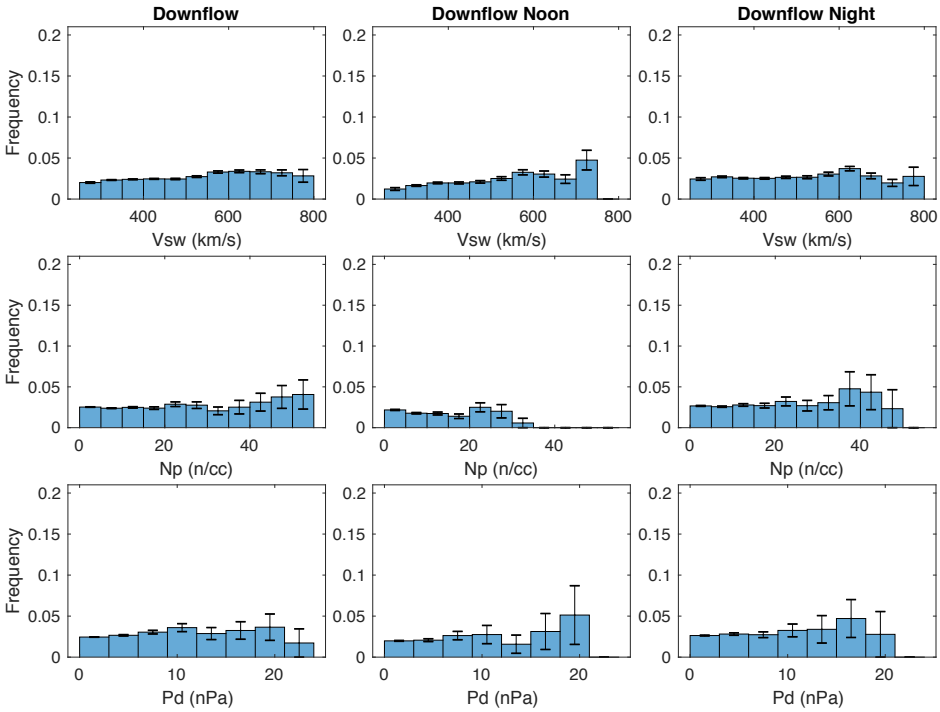

Figure S11. Ion downflow occurrence frequencies plotted over solar wind parameters, in the same format as ion upflow (Figure S10).

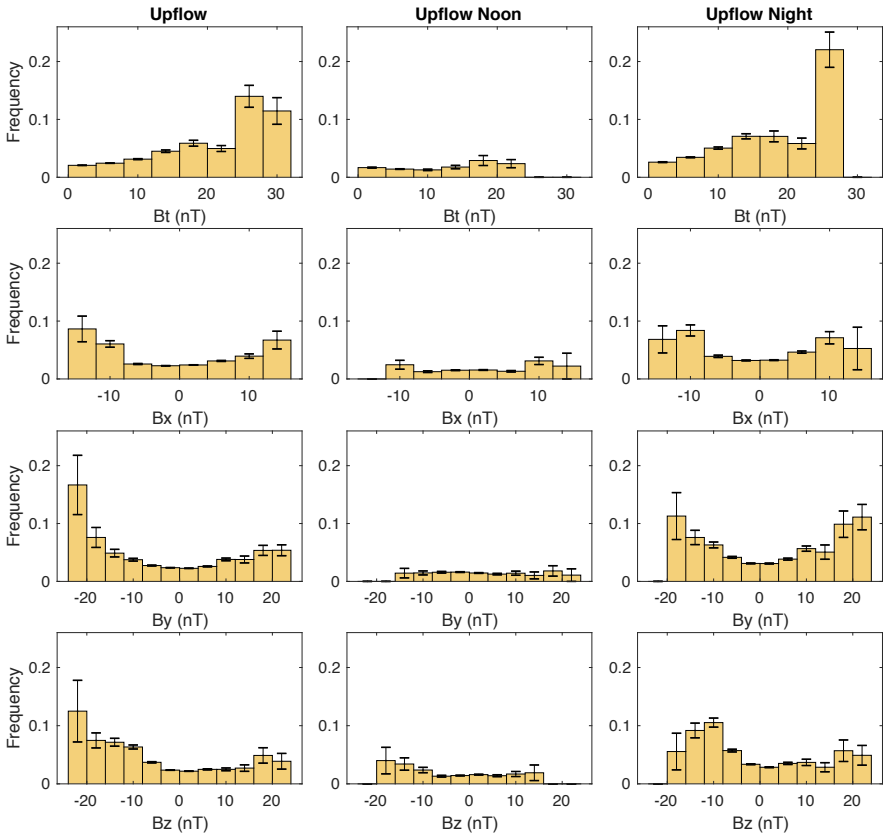

Figure S12. Ion upflow occurrence frequency plotted over the IMF components: total IMF (first row), IMF Bx (second row), IMF By (third row), IMF Bz (fourth row), for different MLT

intervals: Over all MLT (first column), on the dayside between 9 – 15 MLT (second column), on the night side between 21 – 3 MLT (third column).

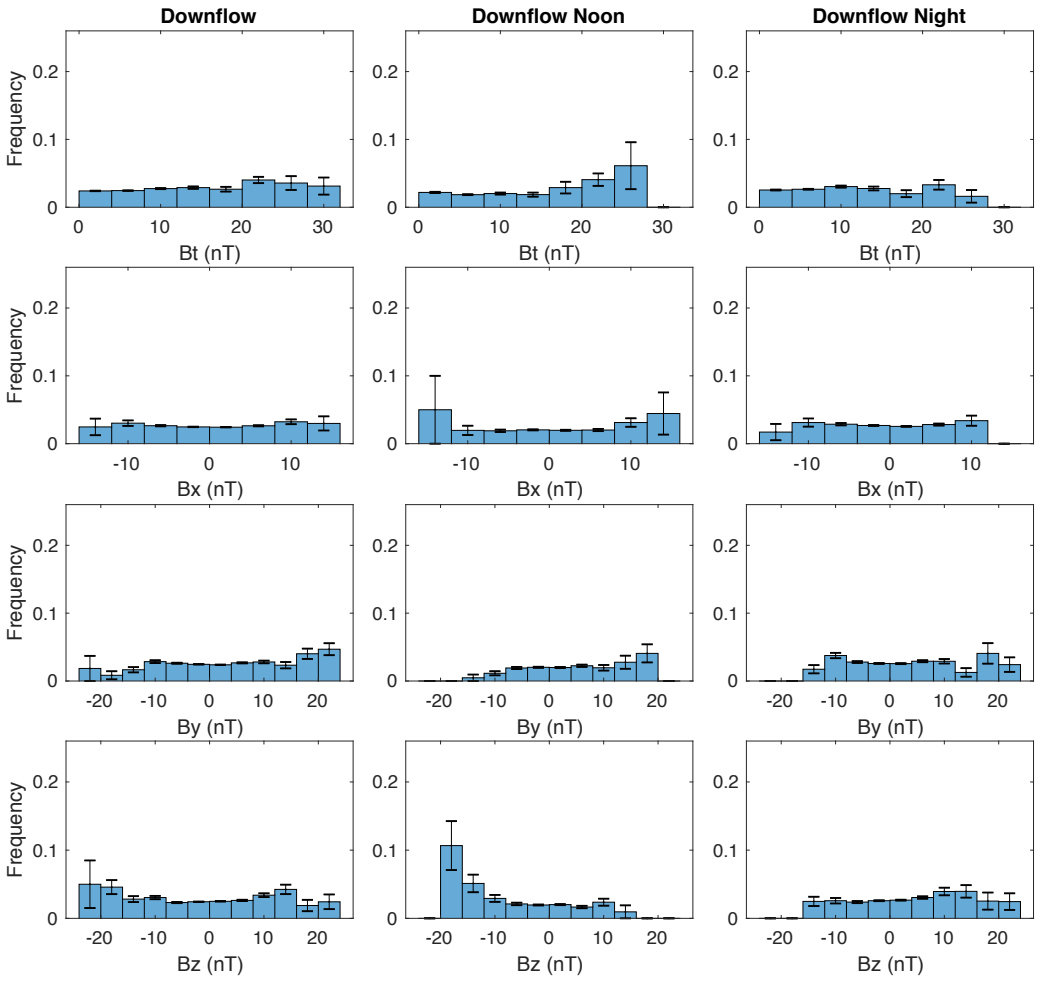

Figure S13. Ion downflow occurrence frequency plotted over the IMF components, with the same format as the ion upflow (Figure S12)

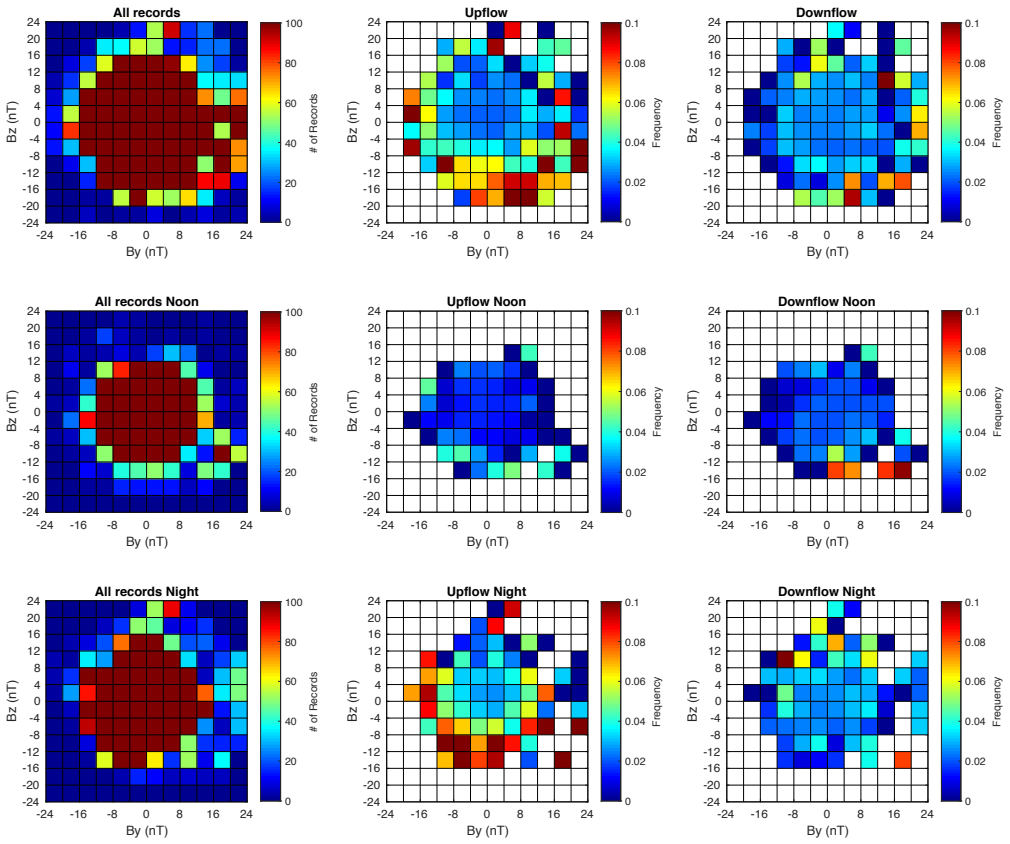

Figure S14. Heatmaps showing joint distributions of ion upflow/downflow occurrence frequency on the IMF By and IMF Bz components. Each row represents a certain MLT sector: overall MLT (first row), on the dayside between 9 – 15 MLT (second row), on the night side between 21 – 3 MLT (third row). The first column indicates total count of records in each bin, while the second and third columns show distributions of upflow and downflow occurrence frequency, respectively.